

Overview of Quasi Single Helicity Experiments in Reversed Field Pinches

P. Martin, L. Marrelli, G. Spizzo, P. Franz, P. Piovesan, I. Predebon, T. Bolzonella, S. Cappello, A. Cravotta, D.F. Escande, L. Frassinetti, S. Ortolani, R. Paccagnella, D. Terranova and the RFX team,

Consorzio RFX, Associazione Euratom-Enea sulla fusione, Padova, Italy

B.E. Chapman, D. Craig, S.C. Prager, J.S. Sarff and the MST team,

Department of Physics, University of Wisconsin-Madison, Madison, Wisconsin, USA

P. Brunzell, J.-A. Malmberg, J. Drake and the EXTRAP T2R team,

Division of Fusion Plasma Physics, Royal Institute of Technology, Association Euratom-VR, Stockholm, Sweden

Y. Yagi, H. Koguchi, Y. Hirano and the TPE-RX team,

National Institute of Advanced Industrial Science and Technology (AIST), Tsukuba, Japan

R.B. White,

Princeton Plasma Physics Laboratory, Princeton, NJ, USA

C. Sovinec,

Center for Plasma Theory and Computation, University of Wisconsin-Madison, Madison, Wisconsin, USA

C. Xiao,

University of Saskatchewan, Canada

R.A. Nebel,

Los Alamos National Laboratory, Los Alamos, NM, USA

D.D. Schnack,

Science Applications International Corporation, San Diego, CA, USA

e-mail contact of main author: martin@igi.pd.cnr.it

Abstract. We report the results of an experimental and theoretical project dedicated to the study of Quasi Single Helicity Reversed Field Pinch plasmas. The project has involved several RFP devices and numerical codes. It appears that QSH spectra are a feature common to all the experiments.

1. Introduction

In the last years the Reversed Field Pinch (RFP) [1] community has concentrated a strong effort on tasks dedicated to the control of magnetic turbulence [2]. An approach to a less chaotic RFP configuration is based on the theoretical prediction that the RFP plasma can spontaneously access, through a self-organization process, the Single Helicity (SH) regime [3,4]. In this condition the dynamo needed to sustain the RFP configuration is driven by an individual $m=1$ instability. The SH state would naturally be resilient to the magnetic chaos implicit in the standard multi-mode (Multiple Helicity-MH) dynamo and this is therefore beneficial for plasma confinement.

The possibility of having a RFP plasma in a pure SH state was put forward since 1983 through two-dimensional numerical simulations (see [4,5] for a collection of references) where a stationary RFP state was found by forcing SH. Later, the existence of a bifurcation from MH to SH was proved in fully 3D simulations [6,7,8] and has recently been discussed

as controlled by the Hartmann number $H_\infty(v\eta)^{-1}$, where η and v are the plasma resistivity and viscosity respectively [5]. The SH states are not the helical Taylor states [4]. On the experimental side, since 1994 results have been reported in several machines where the plasma was transiently in a quasi-SH (QSH) state [9,10,11,12]. Stationary QSH spectra have been discovered in RFX [3], where, in this regime, a coherent helical structure in the plasma core with closed magnetic flux surfaces has been detected. QSH states are the closest experimental approximation of the theoretical SH states: QSH differs from SH mainly because of the nature of magnetic spectra of $m=1$ modes. While one $m=1$ mode dominates the QSH spectra, the other modes (so called “secondary”) still have non-zero amplitude and therefore contribute to the production of residual magnetic chaos outside the helical domain.

Given the potential benefit of a self-organized, non-chaotic RFP configuration we have started an experimental and theoretical project, which involves several RFP devices and numerical codes. This initiative is devoted to collect and organize all the QSH evidence in a unique database to study QSH in a variety of

Device	R/a (m)	Plasma current achieved/design (kA)	Vertical field penetration time (ms)
EXTRAP T2R	1.24/0.183	100/300	≈ 6 ms
TPE RX	1.72/0.45	500/1000	≈ 320 ms
MST	1.5/0.52	500/500	≈ 500 ms
RFX	2/0.457	1100/2000	≈ 400 ms

TABLE I

different conditions and to control and optimize this helical regime. In this paper we report the results of this effort. Experiments have been conducted in four different RFP devices (Table I): EXTRAP T2R at Royal Institute of Technology in Stockholm [13], TPE-RX at AIST in Tsukuba [14], MST at the University of Wisconsin-Madison [15] and RFX at Consorzio RFX in Padova [16]. The codes that have been used for this study are ORBIT [17], NIMROD [18], SPECYL [19] and DEBS [20]. ORBIT is a hamiltonian guiding center Monte Carlo code with numerical or analytic equilibria. NIMROD is a 3D MHD code capable to work with generic geometry, while SPECYL and DEBS are 3D cylindrical MHD codes.

2. The QSH experimental picture

QSH plasmas have been studied with a variety of diagnostics. Standard MH spectra of $m=1$ instabilities in RFP's, measured by pick-up coils, are composed by many modes with various toroidal mode numbers $n \geq 2 \cdot R/a$ [1]. The spectrum is usually peaked around the lowest values of n ($n \approx 2 \cdot R/a$) and in MH conditions several modes have comparable amplitudes, though $m=1$ modes amplitude rapidly decreases for increasing n . QSH spectra are characterized by the presence of one ($m=1, n=n_D$) dominant mode. Its amplitude is typically several times larger than those of the secondary modes. The ratio between the dominant and the secondary modes amplitudes varies depending on the device and is also a function of the plasma conditions, but values ≥ 3 are typically characterizing QSH spectra. It is customary to describe the width of the toroidal spectrum of $m=1$ modes by means of

the N_s parameter, defined as $N_s = \left[\sum_n \left(\frac{W_n}{\sum_{n'} W_{n'}} \right)^2 \right]^{-1}$, where W_n is the energy of the ($m=1, n$) mode. A pure SH spectrum corresponds to $N_s=1$.

Reproducible experimental evidence of spontaneous QSH spectra has been observed in three devices, RFX, MST and TPE-RX, while QSH has been detected only sporadically in EXTRAP T2R. For these devices typical time traces of the ($m=1,n$) modes amplitudes normalized to the edge poloidal magnetic field are shown in Figure 1 (for RFX and TPE-RX the toroidal component of magnetic fluctuation is reported, for MST and EXTRAP T2R the poloidal). This figure shows some important features about the time evolution and the purity of QSH spectra. QSH spectra lasting throughout the discharge are observed in RFX and TPE-RX (Fig. 1-A and 1-B), while in MST they are typically transient, though lasting for a significant fraction of the plasma pulse (Fig. 1-C). In these three devices, anyway, the duration of QSH conditions is longer than the standard energy confinement time. In MST the purest spontaneous QSH spectra have been recorded (with the ratio between dominant and secondary modes amplitude >10) and a redistribution of the energy between the various modes is observed [21]: the increase of the dominant mode is accompanied by the decrease of secondary modes amplitude. A consistent result is obtained also in TPE-RX: Figure 2 shows the behavior of the dominant mode amplitude (Fig. 2-A) and of that of secondary modes (Fig. 2-B) for TPE-RX. Each point corresponds to an average over several reproducible discharges. In EXTRAP T2R (Fig. 1-D) QSH is observed rarely, and it usually lasts for a short time, though some examples of long-lasting QSH spectra are found. A wide plasma parameter scan has still to be performed in this device.

These external magnetic fluctuation measurements are representative of a significant modification of the plasma core. Soft x-ray (SXR) tomographic imaging [3] reveals that the dominant mode produces a helical coherent structure with closed helical flux surfaces and the same pitch as the dominant magnetic mode. SXR tomography was available in RFX [22] and MST [23], where maps of SXR

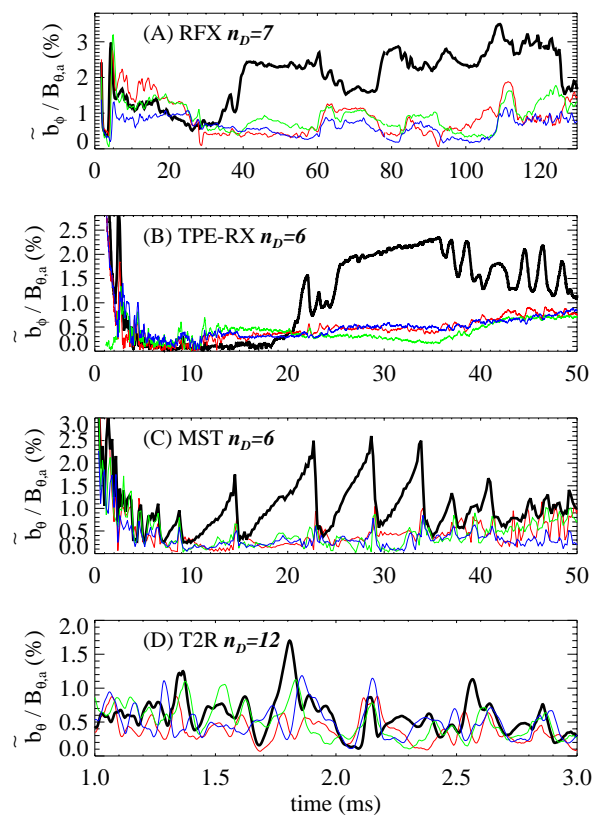


Figure 1: time evolution of four ($m=1,n$) modes for each device. RFX: $n=7$ to 10. TPE-RX: $n=6$ to 9. MST: $n=5$ to 8. T2R $n=11$ to 14. Dominant mode in black curve.

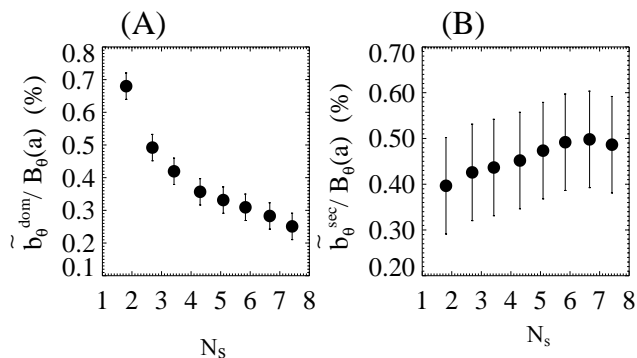


Figure 2

maps of SXR

emissivity taken in MH and in QSH plasma are rather different [22]. A poloidally symmetric emissivity is found in the MH state. This is consistent with a region of strong heat transport in the plasma core, as one could expect because of the presence of a stochastic magnetic field. In contrast a bean-like hot $m=1$ structure is evident in the QSH case. The location of the structure systematically coincides with the resonance radius and poloidal phase angle of the dominant $m=1$ mode, which are reconstructed from magnetic measurements [22]. A typical example of coherent structure imaging in MST is reported in Fig. 3. This Figure shows the island when, due to its rotation, it is located at the Low Field Side (Fig. 3-A) and at the High FS (Fig. 3-B) of the torus, respectively. The different size of the island on the LFS and HFS is due to toroidal effects, which are directly detected in MST with FIR polarimetry [24]. We notice that the structure extends radially for a significant fraction of the minor radius. These results show that an increased energy stored in magnetic fluctuations does not necessarily mean magnetic stochasticity: the transition from chaos to order is also controlled by the energy distribution among the various modes. This is confirmed by the magnetic flux surfaces analysis performed with the ORBIT code. Fig. 4 shows a Poincaré plot in the poloidal cross section calculated for a MST QSH spectrum with $n_D=6$, corresponding to the same 400 kA shot as in Fig. 3: a coherent structure emerges from magnetic chaos. For this Poincaré plot the radial magnetic perturbation \tilde{b}_r has been calculated from Newcomb's equation. For the case shown in the figure this leads to a peak amplitude of the radial magnetic field fluctuation associated to the dominant mode of $\approx 0.01B(0)$, i.e. $\approx 6\text{mT}$.

As a final point, it is worth noting the beneficial effects of QSH spectra on the mode wall-locking problem, which affects in particular RFX and TPE-RX. In RFX, where in MH conditions modes are always strongly locked, the strength of phase correlation between $m=1$ modes is reduced in QSH conditions, as shown in Fig. 5, where the distribution of locking strength values L_S is reported for MH and QSH plasmas [25]. L_S is defined as the normalized sum over the main

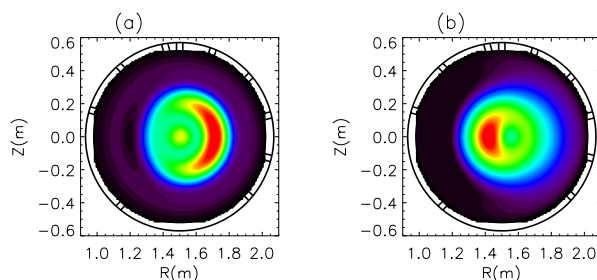


Figure 3

its rotation, it is located at the Low Field Side (Fig. 3-A) and at the High FS (Fig. 3-B) of the torus, respectively. The different size of the island on the LFS and HFS is due to toroidal effects, which are directly detected in MST with FIR polarimetry [24]. We notice that the structure extends radially for a significant fraction of the minor radius. These results show that an increased energy stored in magnetic fluctuations does not necessarily mean magnetic stochasticity: the transition from chaos to order is also controlled by the energy distribution among the various modes. This is confirmed by the magnetic flux surfaces analysis performed with the ORBIT code. Fig. 4 shows a Poincaré plot in the poloidal cross section calculated for a MST QSH spectrum with $n_D=6$, corresponding to the same 400 kA shot as in Fig. 3: a coherent structure emerges from magnetic chaos. For this Poincaré plot the radial magnetic perturbation \tilde{b}_r has been calculated from Newcomb's equation. For the case shown in the figure this leads to a peak amplitude of the radial magnetic field fluctuation associated to the dominant mode of $\approx 0.01B(0)$, i.e. $\approx 6\text{mT}$.

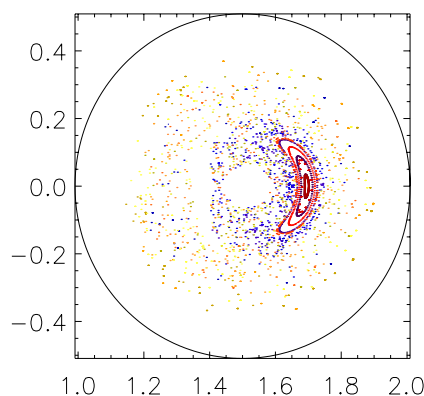


Figure 4: x- and y-axis units in (m)

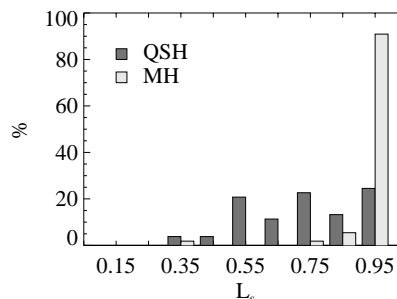


Figure 5

locking strength values L_S is reported for MH and QSH plasmas [25]. L_S is defined as the normalized sum over the main

interacting modes of the cosine of their phase difference $L_S \propto \sum_{n1,n2} \cos(\varphi_{n1} - \varphi_{n2})$. A perfect

phase locking gives a value of L_S equal to 1, while a complete decorrelation gives a value equal to 0. The reduction of phase locking is often associated to the onset of a spontaneous rotation of one or two $m=1$ modes, typically with n numbers close to that of the dominant one. This is due to a redistribution of the magnetic energy between the various normal modes as a result of the MH to QSH transition and to a modified non-linear interaction between modes [25].

3. Velocity and magnetic fluctuations during QSH

Numerical simulations indicate that a RFP configuration can be sustained with a single $m=1$ mode in a pure SH state. Although this condition has not been achieved experimentally, it is important to determine whether the dominant mode in QSH plasmas produces significant dynamo fields of the form $\langle \tilde{v} \times \tilde{b} \rangle$, where $\langle \dots \rangle$ represents a flux surface average. Previous work in MST reported that in standard MH sawtoothing plasmas, dynamo action was large only during sawtooth crashes, where large amplitude magnetic and velocity fluctuations were coherent and in the proper phase to produce a $\langle \tilde{v} \times \tilde{b} \rangle$ electric field [26].

Plasma flow velocity fluctuations \tilde{v} have been measured in MST at 300 kA, far from sawtooth events, with Doppler spectroscopy [27] along several poloidal and toroidal lines of sight. By correlating \tilde{v} measurements with mode resolved edge magnetic field fluctuations, the coherent part of the velocity fluctuations associated with individual $(1,n)$ modes has been isolated. This is shown in Fig. 6. Here the contribution from the $n=6$ mode (triangles) during QSH (Fig. 6-a) and MH (Fig. 6-b) is compared to the average from all of the secondary modes (squares). We observe that the velocity fluctuation for the dominant $n=6$ mode increases during QSH, in coincidence with the increase in magnetic fluctuation amplitude for the same mode. Also, the velocity fluctuation for other modes stays the same or decreases in QSH. This implies that the velocity fluctuations have achieved a narrower spectrum in a similar way to the magnetic fluctuations, whose ensemble averaged spectra in QSH and MH conditions for the same group of shots are shown in Figs. 6-c and 6-d respectively. Work is continuing on extracting the dynamo product $\langle \tilde{v} \times \tilde{b} \rangle$ from these data. However, it seems likely that the dynamo produced by the dominant $n=6$ mode will be significantly larger during QSH than what is observed away from sawteeth in MH.

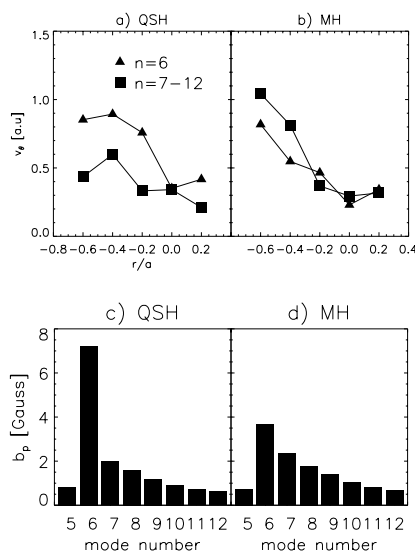


Figure 6

4. QSH experimental control parameters

The large datasets of reproducible discharges obtained in the four devices has enabled a statistical analysis of QSH spectra, and the search for their experimental control parameter. Numerical studies show that the MH-SH transition is ruled by the Hartmann number H .

Given the difficulty of an accurate measurement of plasma viscosity, a direct comparison with the theory is very difficult. Therefore we concentrated on experimental global plasma control parameters. Analysis performed in MST [21], RFX [25] and TPE-RX shows some common trends. In all three devices we observe a trend for an increased probability of obtaining QSH spectra when current is raised. Figure 7-A shows the probability density function $p(N_s)$ of N_s values for different values of plasma current in TPE-RX. $p(N_s)$ is normalized such that $\int p(N_s) dN_s = 1$. Low values of N_s are more likely at the higher current levels.

Not only the absolute value of the plasma current, but also its time evolution might influence the spectral shape. We know in fact that a QSH spectrum is achieved in numerical simulations during current ramp-down experiments [28]. The shape of the magnetic equilibrium and in particular the amount of edge magnetic toroidal field reversal also influences the probability of obtaining QSH spectra: QSH spectra

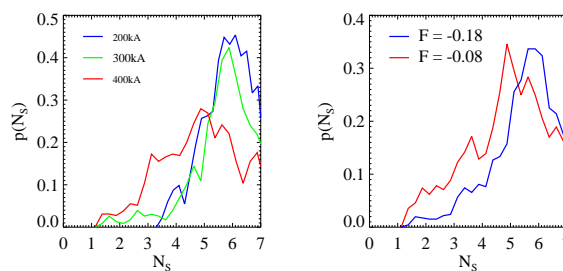


Figure 7

are more frequently observed in discharges with shallow reversal, as indicated in Fig. 7-B, where the $p(N_s)$ function is shown for two different values of $F = B_\phi(a) / \langle B_\phi \rangle$. A similar result is found in RFX [25]. This is consistent with numerical results from SPECYL code applied to RFX geometry: they indicate that at shallow reversal the MH-SH transition threshold (as a function of H) is smoother [29]. This corresponds to a wider QSH transition range with less negative F , which means that in correspondence of H values where at deep F a MH spectrum is still found, QSH spectra are observed at shallower F .

The aspect ratio is also a parameter that influences the shape of the MHD modes spectrum. It is known [30] that the average number of $m=1$ modes in the spectrum depends on the aspect ratio. This might explain the difficulty of obtaining QSH spectra in EXTRAP T2R: there the background standard $m=1$ spectrum is very broad, and the plasma must strongly depart from the standard spectrum in order to get QSH conditions. For the lower aspect ratio MST device, standard spectra are on the average rather narrow.

5. Confinement and stability in finite beta helical states

Experimental measurements [3,31] show that the helical coherent structure is a region of reduced transport. SXR emissivity is stronger and direct measurements show that the electron temperature in the island is indeed larger there than in the surrounding plasma [31]. Given the limited volume of the helical structure (for example in RFX up to 10% of the total plasma volume), the global confinement is not strongly affected. It is worth noting that in MST, where the purest QSH spectra are obtained and the more marked reduction of secondary modes is recorded, an increase of SXR emission in correspondence with QSH spectra is observed [21].

In order to model the observed confinement changes in QSH spectra and to predict what would happen if a pure SH could be reached, we have performed a study of particle transport with the ORBIT code. This has been done by analyzing the diffusion of test particles (ions) which have been deposited in the plasma core in three different magnetic configurations: MH, QSH and SH (all with the same total magnetic energy stored in $m=1$ modes, but distributed in different ways among the various helicities). To quantify the

transport we have measured the time needed to lose 50% of the particles deposited in the core out from a preset border located at an outer radius. We find that particles deposited inside the helical structure in the QSH case are lost more slowly than those deposited outside it or in a MH plasma. The loss time in the former case is about one order of magnitude longer. A further one order of magnitude improvement with respect to QSH is found with a pure SH spectrum when particles are deposited inside the helical structure. In this case no magnetic chaos is present outside the helical domain.

The pressure gradient maintained in the helical region represents a source of free energy for MHD modes, but the longevity of the temperature distortions suggests that pressure-driven modes may be stable. Although axisymmetric RFP equilibria have bad magnetic curvature everywhere and are therefore susceptible to resistive pressure-driven modes, the helical flux surfaces in SH and QSH states have distinct topologies that resemble stellarator-like configurations.

The finite- β properties of SH and QSH states are being investigated numerically with the NIMROD code [18]. The geometry for the computations is a periodic cylinder to allow the formation of pure SH states, and the parameters $S=2000$ and $Pm=100$ are chosen to produce single helicity, as expected from a study at 0- β [5]. S and Pm are the Lundquist and Prandtl numbers respectively.

With Ohmic heating and anisotropic thermal conduction (leading to internal energy $\approx 15\%$ of the stored energy), the resulting pressure distribution is peaked at the magnetic axis of the helical flux surfaces, which remain intact. The computed temperature distribution (Fig. 8-a) has features that resemble the experimental SXR measurements displayed in Fig. 3. The flux-surface-average magnetic pressure from the simulation (Fig. 8-b) shows the existence of a magnetic well [32] from the helical magnetic axis ($r_0=0.45$) to the separatrix ($r_0=0.68$), where r_0 is a Lagrangian coordinate. Although the well is suggestive of good average curvature, it does not prove MHD stability. The large viscosity needed for SH also affects interchange modes and may be the dominant stabilizing effect in the simulation. Nonetheless, the existence of a well is a favorable topological feature of the helical state that is precluded in axisymmetric RFPs.

6. Conclusions

This joint research program on self-organized helical RFP states has combined the effort of many experimental and theoretical groups. Self-organized QSH spectra are found in all the existing devices: QSH appears therefore to be robust and not dependent on very peculiar boundary conditions. Global plasma parameters, which favor the transition towards QSH spectra, have been identified. In particular it is encouraging the fact that QSH states are experimentally more easily accessible at high plasma current.

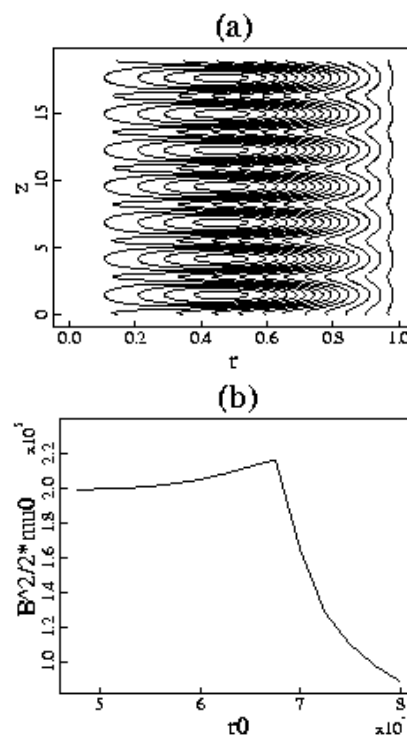


Figure 8

Long lasting QSH states have been found in several experiments. This, along with the experimental hints of a more steady dynamo action provided by the dominant mode as compared to the intermittent nature typical of the MH dynamo, are suggestive signatures of a path towards laminar dynamo field as predicted by pure SH numerical states. Also, the reduced plasma-wall interaction and the observed heating of the helical structure are promising for the future optimization and full exploitation of helical states in RFPs. Numerical simulations show that the good particle confinement properties and the existence of a magnetic well are distinctive features of helical RFPs as compared to the standard axisymmetric mean field profiles with a MH magnetic turbulence.

Although much remains to be done, our results expand and reinforce the evidence that the formation of self-organized states with one dominant helical mode (Ohmic Single Helicity state) is an approach complementary to active control of magnetic turbulence to improve confinement in a steady state RFP.

Acknowledgments. This work is being carried out in the framework of the IEA Implementing Agreement on Reversed Field Pinches.

References

- [1] ORTOLANI S., SCHNACK D.D. “ Magnetohydrodynamics of plasma relaxation”, World Scientific, Singapore (1993)
- [2] SARFF J.S. , et al., this conference, paper OV4-3 (2002)
- [3] ESCANDE D.F. et al, Phys. Rev. Lett., **85**, 1662 (2000).
- [4] ESCANDE D. F. et al Plasma Phys. Contr. Fus. **42**, p.B243-B253 (2000)
- [5] CAPPELLO S. AND ESCANDE D. F., Phys. Rev. Lett. **85**, 3838 (2000).
- [6] CAPPELLO S AND PACCAGNELLA R in *Proc. Workshop on Theory of Fusion Plasmas*, ed E Sindoni (Bologna: Compositori) p 595 (1990).
- [7] CAPPELLO S AND PACCAGNELLA R, Phys. Fluids **B 4**, 611 (1992).
- [8] FINN J M, NEBEL R A, BATHKE C C, Phys. Fluids **B4**, 1262 (1992).
- [9] NORDLUND P and MAZUR S 1994, Phys. Plasmas **1**, 4032
- [10] BRUNSELL P., et al. Phys. Fluids, **5**, 885 (1993).
- [11] SARFF, J S et al., Phys. Rev. Lett. **78**, 62 (1997).
- [12] MARTIN P, Plasma Phys. Contr. Fus. **41**, A247 (1999)
- [13] BRUNSELL P R, et al. Plasma Phys. Control . Fusion **43** (2001) 1457-1470
- [14] YAGI Y. et al. Fusion Eng. and Design **45**, 409 (1999)
- [15] DEXTER R.N. et al., Fusion Technol. **19**, 131 (1991)
- [16] ROSTAGNI G., Fus. Eng. Design **25**, 301, (1995).
- [17] WHITE R.B., Phys Fluids **2**, 845 1990.
- [18] GLASSER A. H., et al., Plasma Phys. Control. Fusion **41**, A747 (1999).
- [19] CAPPELLO S., BISKAMP D. Nucl. Fusion, **36**, 571 (1996).
- [20] SCHNACK D.D. et al., Computer Physics Communications **43**, 17 (1986).
- [21] MARRELLI L. et al. Phys. Plasmas, **9**, 2868, (2002)
- [22] FRANZ P., et al. Nucl. Fusion **41**, p. 695-709 (2001).
- [23] FRANZ P. et al., to be published in Rev. Sci. Instrum (2002).
- [24] BROWER D. this conference , paper EX/C4-6 (2002).
- [25] BOLZONELLA T., TERRANOVA D., submitted to Plasma Phys. Contr. Fusion (2002).
- [26] FONTANA P.W. et al., Phys. Rev. Lett. **85**, 566 (2000).
- [27] DEN HARTOG D.J., et al., Phys. Plasmas **6**, 1813 (1999).
- [28] NEBEL R., et al. “Self-Similar Decaying Profiles for Reversed-Field Pinches” to be published in Phys. Plasmas (2002).
- [29] CAPPELLO S. et al., 28th EPS Conf Contr. Fus. and Plasma Phys, **25A** 1553-1556 (2001).
- [30] HO W. et al Phys. Plasmas **2**, 3407 (1995).
- [31] MARTIN P., et al., Phys. Plasmas **7**, p. 1984-1992 (1999).
- [32] MILLER G., *Phys. Fluids*, **B1**, 384 (1989).